

## Supporting Information

### Facile Gelation of Fully Polymeric Conductive Hydrogel Activated by Liquid Metal Nanoparticles

*Ming Wang,<sup>a</sup> Xiao Feng,<sup>a</sup> Xijun Wang,<sup>a</sup> Songnan Hu,<sup>a</sup> Cunzhi zhang,<sup>a</sup> Haisong Qi\*<sup>a</sup>*

<sup>a</sup> State Key Laboratory of Pulp and Paper Engineering, South China University of Technology, Guangzhou 510641, China

Corresponding author.  
E-mail: qihs@scut.edu.cn

Keywords: Liquid metal nanoparticles, PEDOT: bacterial cellulose nanofiber, free radical polymerization, self-healing, force mapping.

#### Supplementary data

AFM images and Zeta potential of sulfamic acid-mediated BCNFs, <sup>1</sup>H NMR spectra, FT-IR spectrum, LPBP hydrogel without APS and crosslinkers, weekly cross-linked stage, LMNPs in hydrogel, 3D porous structure, mechanical strength, rheological amplitude strain scan, compression curves, electrical conductivity, stability, sensory to handwriting, transmittance.

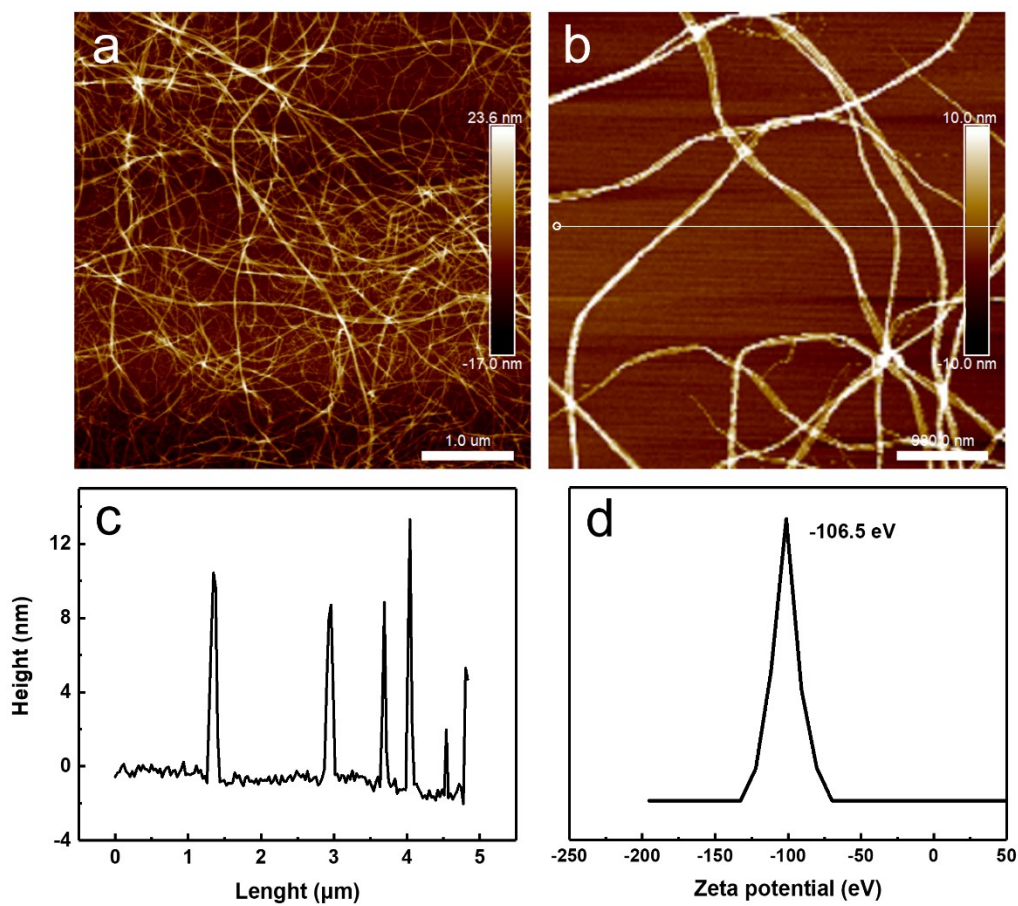


Figure S1. a, b)AFM and c)its height images of sulfamic acid-mediated BCNFs. D) Zeta potential of sulfamic acid-mediated BCNFs at pH of 7.

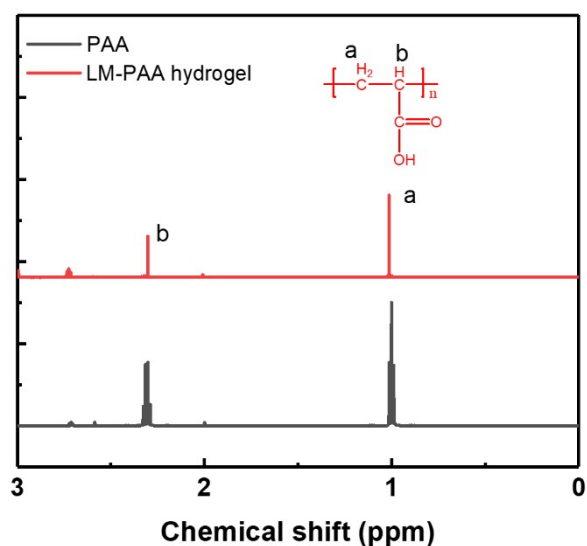


Figure S2.  $^1\text{H}$  NMR spectra (400 MHz) of LM-PAA hydrogel, deuterioxide ( $\text{D}_2\text{O}$ ) was used as external reference. The characteristic peaks in the  $^1\text{H}$  NMR spectrum (methylene protons  $\sim 1.01$  ppm and methine protons  $\sim 2.30$  ppm) indicated the presence of the PAA.

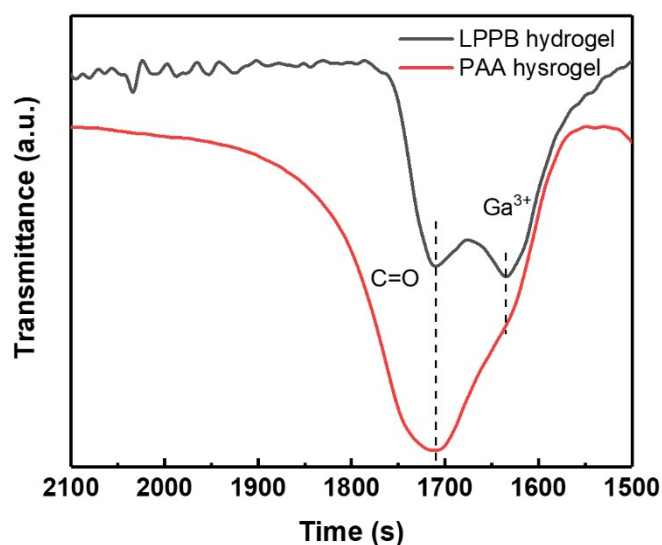


Figure S3. FT-IR spectrum of the LPPB hydrogel and pure PAA hydrogel. The appearance of the new peak at  $1634\text{ cm}^{-1}$  verified the coordinate bonds between  $\text{Ga}^{3+}$  ions and carboxyl groups.

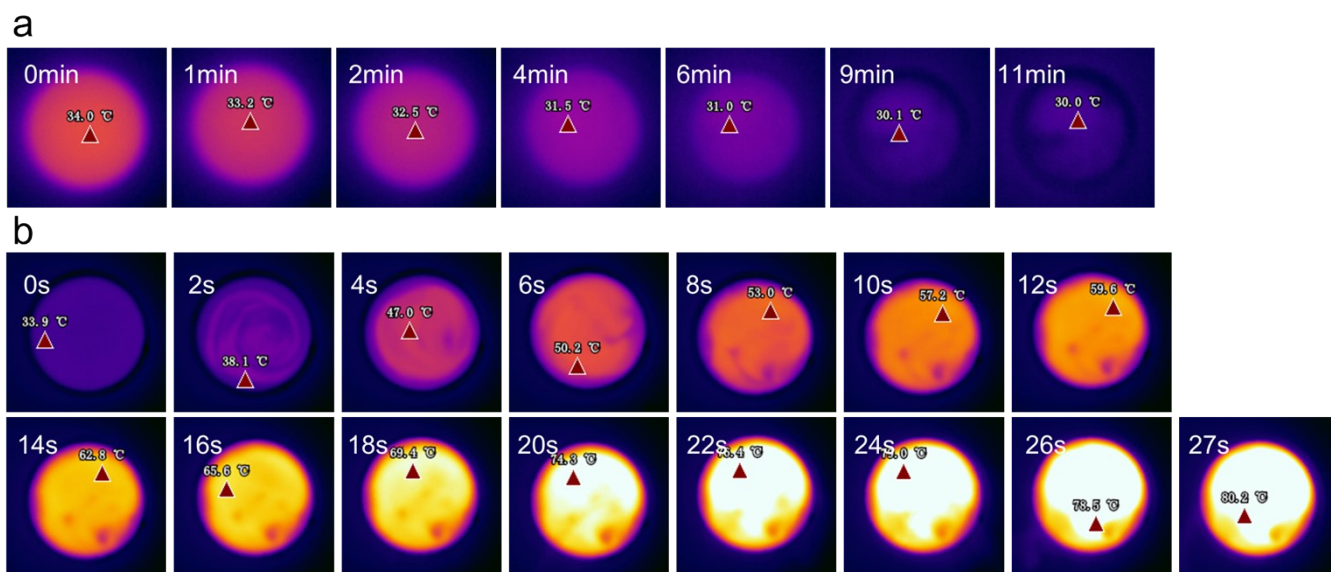


Figure S4. More details of the temperature changes of a) LM-PEDOT:BCNF-AA and b) LM-PEDOT:BCNF-AA-APS.

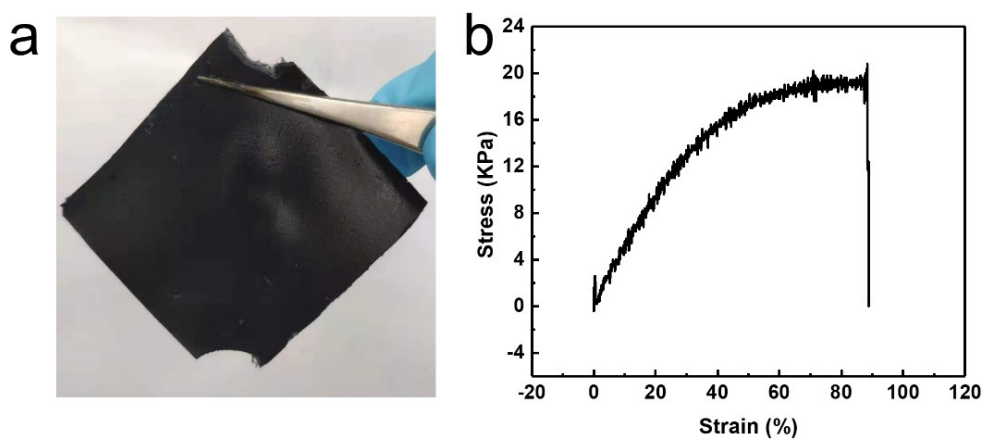


Figure S5. a) LPBP hydrogel without APS and crosslinkers. b) It showed a poor mechanical strength. Incubation time: 72 hours.

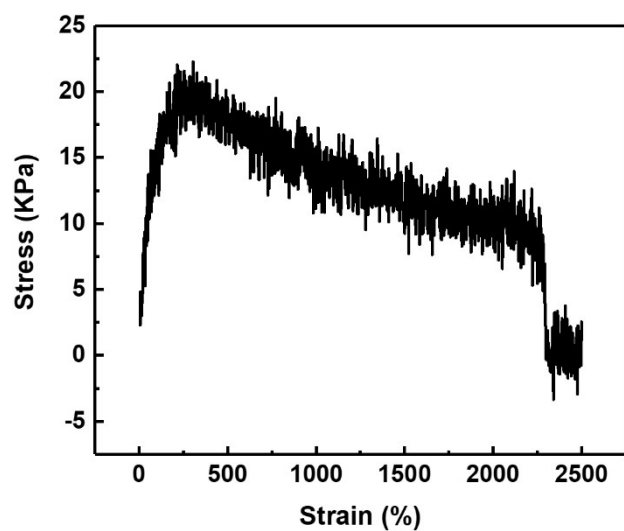


Figure S6. Tensile stress-strain after gelling for 30 min. EGaIn: 1.0 wt%. AA: 25.0 wt%.

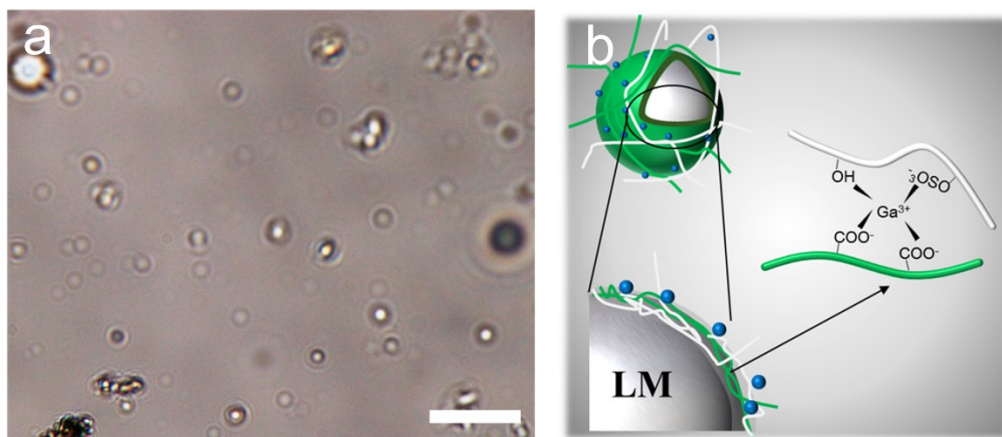


Figure S7. a) Optical microscope image of the surface of LPBP hydrogel. Scale bar:  $5\mu\text{m}$ . b) Schematic diagram of LM nanodroplets in the matrix.

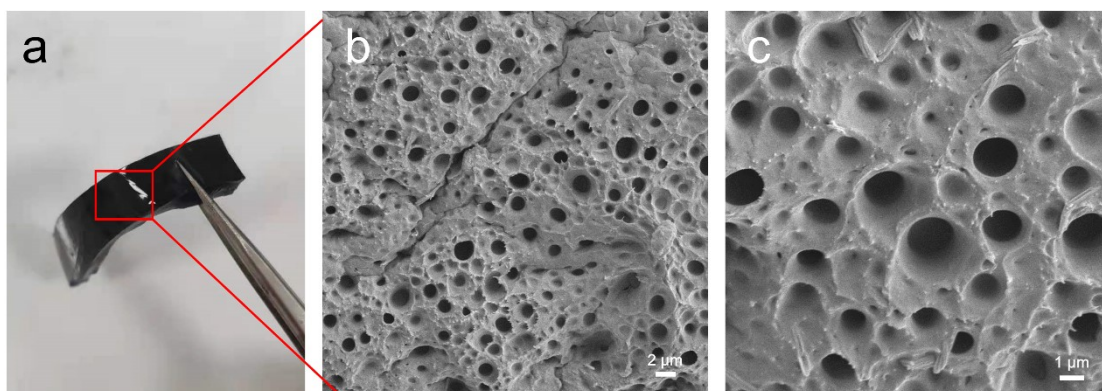


Figure S8 a) Photograph of the LPBP hydrogel. b, c) SEM images of the freeze-dried the LPBP hydrogel.

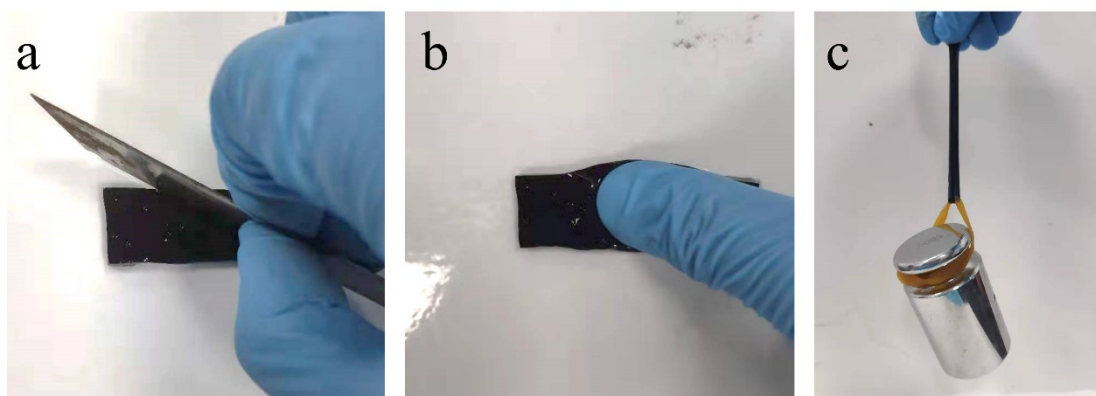


Figure S9. Digital image of LPBP hydrogel a) being cut, b) pressed, and c) hanging metallic weight of 500 g with this elastomer. Incubation time: 24 hours.

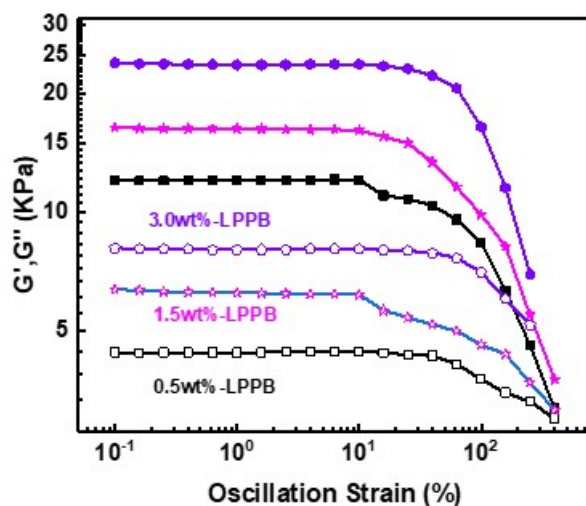


Figure S10. Rheological amplitude strain scan of storage modulus ( $G'$ , solid symbol) and loss modulus ( $G''$ , open symbol) of LPBP hydrogel with different LM concentration content at 25 °C.

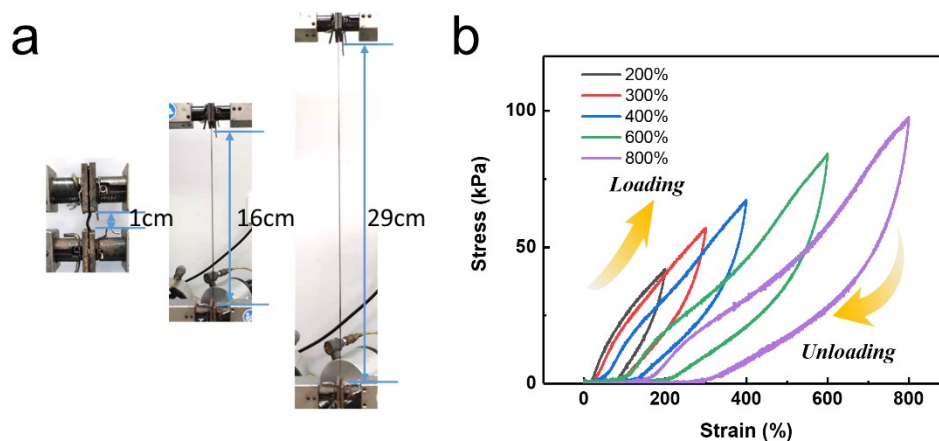


Figure S11. a) Digital images of LPBP hydrogel with 1.5 wt% LM content under uniaxial tensile test. It was able to be stretched up to 28 times its original length, demonstrating the super stretchable properties of LPBP hydrogel. b) Cyclic tensile curves with higher different strains.



Figure S12. a) Photos of 1.5wt% LPBP hydrogel with compressions with 40% strain. b) Successive compression curves at a strain of 40%.

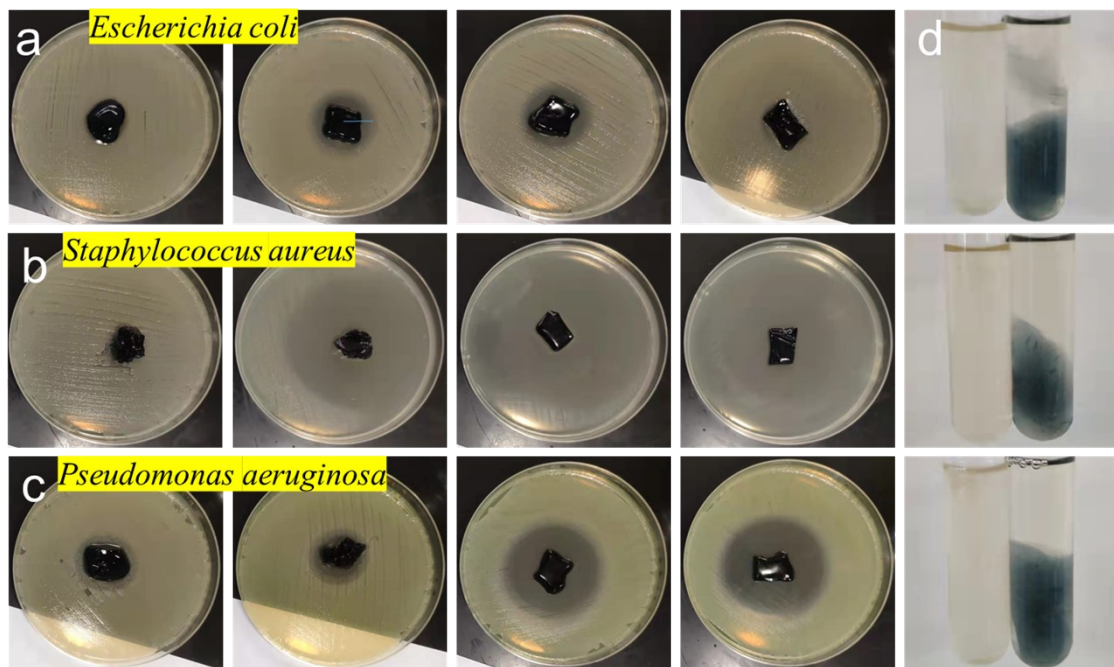


Figure S13. Antibacterial activity of LMBP hydrogel to a) *Escherichia coli*, b) *Staphylococcus aureus* and c) *Pseudomonas aeruginosa* on the plates. And d) in liquid medium.



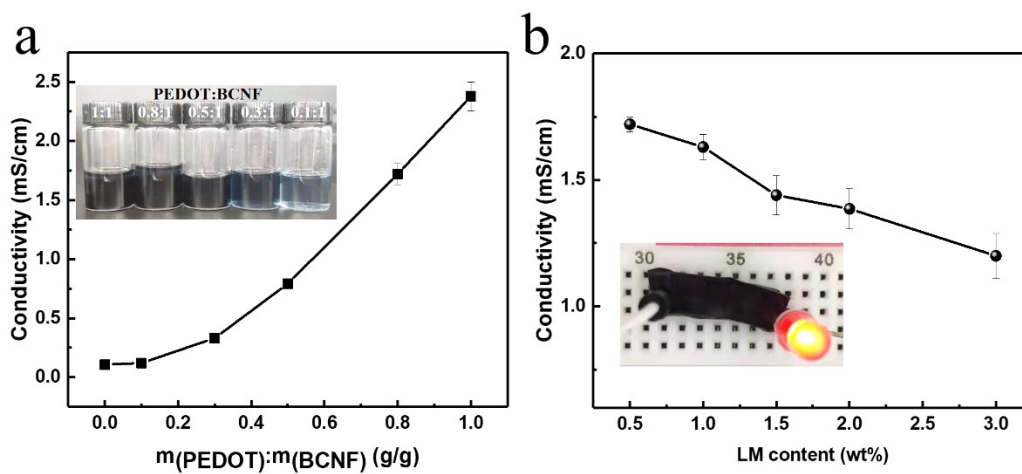


Figure S14. a) Electrical conductivity of LPBP hydrogel with different mass ratios of PEDOT:BCNF and b) with different LM content.

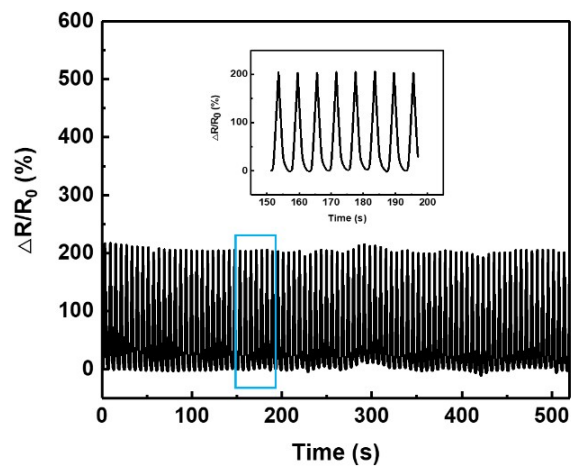


Figure S15. Change in resistance of the strain sensor over 500 stretch-release cycles with a fixed strain of 100% strain.

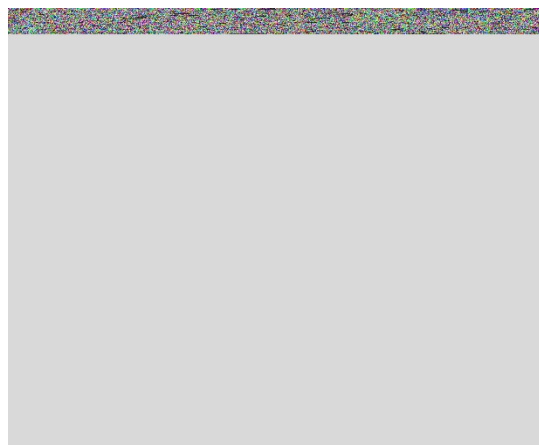


Figure S16. LPBP hydrogel sandwiched by two PET film, this sensor can recognize specific handwriting.

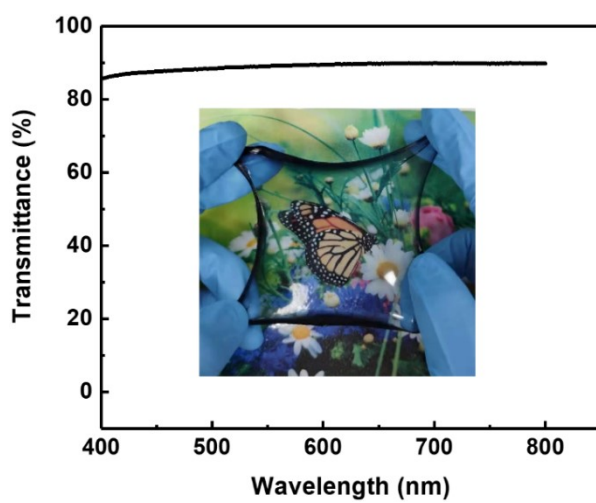


Figure S17. The thin LPBP hydrogel film ( $<0.65\text{mm}$ ) shows high transparency ( $>90\%$  transmittance) in the visible range.